

FT-IR, RAMAN, AND NMR SPECTROSCOPY AND DFT THEORY OF GLIMEPIRIDE MOLECULE AS A SULFONYLUREA COMPOUND****T. Özdemir^{1*}, H. Gökce²**

¹ *Bartın University, Vocational School of Health Services, 74100 Bartın, Turkey; e-mail: tozdemir@bartin.edu.tr, tuba2111@gmail.com*

² *Giresun University, Vocational School of Health Services, 28200 Giresun, Turkey*

The glimepiride molecule was experimentally characterized using vibrational (FT-IR and laser-Raman) and NMR chemical shift spectroscopy. The molecule optimized structure, vibrational wavenumbers, and ¹H and ¹³C NMR isotropic chemical shifts were theoretically obtained with the DFT/B3LYP method at a 6-311++G(d,p) basis set. The theoretical geometric parameters, vibrational wavenumbers, and NMR chemical shifts were found to be consistent with experimental data and similar spectral results in the literature.

Keywords: *glimepiride, vibrational spectrum, ¹H and ¹³C NMR chemical shifts, DFT/B3LYP/6-311++G(d,p) level.*

ИК-ФУРЬЕ, КР И ЯМР-СПЕКТРОСКОПИЯ И РАСЧЕТ МЕТОДОМ ФУНКЦИОНАЛА ПЛОТНОСТИ МОЛЕКУЛЫ ГЛИМЕПИРИДА КАК КОМПОНЕНТА СУЛЬФОНИЛМОЧЕВИНЫ**T. Özdemir^{1*}, H. Gökce²**

УДК 535.375.5;539.143.43

¹ *Бартинский университет, Профессиональная школа медицинских услуг, 74100 Бартин, Турция; e-mail: tozdemir@bartin.edu.tr, tuba2111@gmail.com*

² *Университет Гиресуна, Профессиональная школа медицинских услуг, 28200 Гиресун, Турция*

(Поступила 13 марта 2017)

Методами колебательной (ИК-Фурье, КР) и ЯМР спектроскопии измерены характеристики молекулы глимепирида. Структура молекулы глимепирида, ее колебательные частоты и изотропные химические сдвиги ЯМР ¹H и ¹³C рассчитаны методом функционала плотности DFT/B3LYP с базисным набором 6-311++G(d,p). Полученные результаты согласуются с измеренными данными и результатами других авторов.

Ключевые слова: *глимепирид, колебательный спектр, химические сдвиги ¹H и ¹³C ЯМР, метод DFT/B3LYP/6-311++G(d,p).*

Introduction. Diabetes mellitus is a chronic metabolic disorder, associated with absolute or relative shortage in insulin secretion from the beta cells of pancreas and desensitization of insulin receptors. Patients suffering diabetes need continuous care due to insufficient carbohydrate, fat and protein amounts in their body as a result of insufficient insulin or insulin based defects [1, 2]. Diabetes mellitus is characterized by hyperglycemia resulting from insulin secretion, insulin action, or both [3]. Permanent neonatal diabetes is caused by glucokinase deficiency, and it is an inborn error of the glucose-insulin signaling pathway [4].

Sulfonylureas constitute a class of organic compounds used in medicine. These anti-diabetic drugs are used in the management of diabetes mellitus type 2, and they are classified as first, second, and third generation agents [5, 6]. Glimepiride is an oral anti-diabetic drug from the sulfonylurea group and it is usually used in the treatment of type 2 diabetes mellitus [7–12].

** Full text is published in JAS V. 85, No. 3 (<http://springer.com/10812>) and in electronic version of ZhPS V. 85, No. 3 (http://www.elibrary.ru/title_about.asp?id=7318; sales@elibrary.ru).

Arumugam et al. [13] evaluated various medicinal plants used for antidiabetic activity and diabetes mellitus. Remko [14] used the methods of theoretical chemistry to elucidate molecular properties of the hypoglycemic sulfonylureas and glinides (acetoexamide, tofazamide, tolbutamide, chlorpropamide, gliclazide, glimepiride, glipizide, glibenclamide, nateglinide, and repaglinide). The geometry and energy of these drugs were computed using the Becke3LYP/6-311G(d) method. Karakaya et al. [15] investigated the experimental and theoretical harmonic vibrational frequencies of gliclazide molecule. Crystals of glimepiride were grown by diffusing ethanol into a chloroform solution of glimepiride at room temperature. The stable crystal structure determined by X-ray crystallographic analysis of glimepiride was reported in [16].

1-[[4-[2-(3-Ethyl-4-methyl-2-oxo-3-pyrroline-1-carboxamido)-ethyl]phenyl]sulfonyl]-3-trans-(4-methylcyclohexyl)urea, glimepiride, is a drug used in the treatment of non-insulin dependent diabetes mellitus. The title molecule has several chemical names as given in [17]. The molecular formula, molecular weight and melting point of glimepiride are $C_{24}H_{34}N_4O_5S$, 490.61556 g/mol, and 207°C, respectively [18].

Karakaya et al. [19] investigated the vibrational and structural properties of tolazamide molecule. The geometrical parameters, spectroscopic analysis, vibrational frequencies and quantum chemical calculation of pharmaceutical drug paracetamol (PAR) [20], 4-(3-fluorophenyl)-1-(propan-2-ylidene)-thiosemicarbazone [21], 3-[(4-phenylpiperazin-1-yl)methyl]-5-(thiophen-2-yl)-2,3-dihydro-1,3,4-oxadiazole-2-thione [22], 5-chloro-3-(2-(4-methylpiperazin-1-yl)-2-oxoethyl)benzo[d]thiazol-2(3H) [23], dopamine and amphetamine molecules [24], 1-(2-chloro-4-phenylquinolin-3-yl) ethanone (CPQE) [25] and (\pm)-1,3-dimethyl-5-(1-(3-nitrophenyl)-3-oxo-3-phenylpropyl)pyrimidine-2,4,6(1H,3H,5H)-trione [26] and the 5-(3-pyridyl)-4H-1,2,4-triazole-3-thiol molecule ($C_7H_6N_4S$) [27] were studied using the DFT method.

In the present study, the vibrational wavenumbers and 1H and ^{13}C NMR chemical shifts of glimepiride were experimentally and theoretically studied. The recorded experimental data (FT-IR, laser-Raman, NMR chemical shifts, and bond lengths and angles obtained by X-ray analysis) were supported with parameters computed using theoretical methods (DFT/B3LYP/6-311++G(d,p) level). The obtained theoretical and experimental results were used to give detailed information of the molecular electronic structure of glimepiride. Furthermore, the dipole moment of glimepiride was investigated with the aforementioned computational level.

Experimental. Glimepiride was purchased from Sigma-Aldrich Corporation. The FT-IR spectrum of glimepiride molecule was recorded at room temperature in the region of 400–4000 cm^{-1} using a potassium bromide (KBr) pellet, on a Fourier Transform Infrared spectrometer in solid phase of the sample. The laser-Raman spectrum was recorded at room temperature in the region of 100–4000 cm^{-1} using a RENISHAW Spectrophotometer in Via Raman Microscope. The 785 and 514 nm lines of a diode laser were used as an exciting light for the Laser-Raman spectrum.

The 1H and ^{13}C NMR chemical shift spectra of the compound solved in dimethyl sulfoxide (DMSO- d_6) were recorded with TMS as internal standard using a Premium Compact NMR device at 600 MHz frequency and 14.1 Tesla field power. The chemical shifts were reported at a ppm level.

Computational procedures. The optimized molecular geometry, vibrational wavenumbers, proton and carbon-13 NMR chemical shifts of the title molecule were computed using the DFT/B3LYP (Becke's three-parameter functional (B3)) combined with the gradient-corrected correlational functional of Lee, Yang, Parr (LYP) method) with the 6-311++G(d,p) basis set [28, 29]. Vibrational wavenumbers, geometric parameters and other molecular properties were performed using the GaussView5 molecular visualization program and Gaussian 09W software on a computing system [30–32].

The Raman activities (S_i) calculated with the Gaussian09 program were subsequently converted to relative Raman intensities (I_i) using the following relationship

$$I_i = \frac{f(v_0 - \nu_i)^4 S_i}{\nu_i [1 - \exp(-h\nu_i / kT)]}$$

where ν_0 is the exciting frequency, cm^{-1} ; ν_i is the vibrational wavenumber of the i^{th} normal mode, cm^{-1} ; h , k are the Planck and Boltzmann constants; c is the speed of light; T is temperature, K; and f is a suitably chosen common scaling factor for all peak intensities [33–36].

Results and discussions. *Geometric structure.* The experimental data obtained by single crystal X-ray diffraction [16] were compared with the calculated results given in Table 1. The optimized structure of the title molecule is given in Fig. 1. The 1-[[4-[2-(3-Ethyl-4-methyl-2-oxo-3-pyrroline-1-carboxamido)-ethyl]phenyl]sulfonyl]-3-trans-(4-methylcyclohexyl)urea molecule consists of 68 atoms and accordingly it has 198 modes of vibrations. In order to determine the correlation between the calculated and experimental [16] molecular geometric parameters, the linear correlation coefficient (R^2) value was found as 0.9849 for bond lengths.

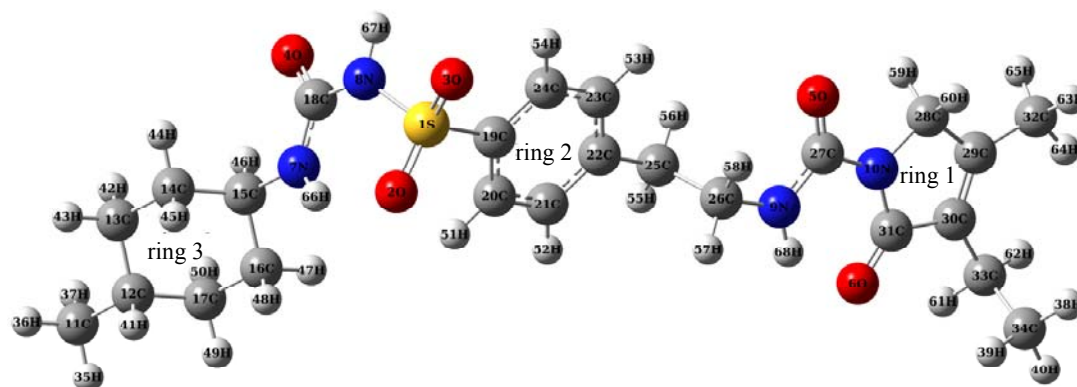


Fig. 1. The optimized molecule structure with the B3LYP/6-311++G(d,p) level of glimepiride.

TABLE 1. The Experimental and Calculated Molecular Geometric Parameters of Glimepiride

Bond length	Experiment [16], Å	Calculated, Å	Bond angles	Experiment [16], degree	Calculated, degree
S(1)-O(2)	1.431 (2)	1.463	O(2)-S(1)-O(3)	119.7 (2)	122.20
S(1)-O(3)	1.420 (2)	1.456	O(2)-S(1)-N(8)	107.80 (10)	106.22
S(1)-N(8)	1.643 (2)	1.691	O(2)-S(1)-C(19)	108.1 (2)	107.95
S(1)-C(19)	1.759 (3)	1.795	O(3)-S(1)-N(8)	105.9 (2)	104.73
O(4)-C(18)	1.230 (3)	1.218	O(3)-S(1)-C(19)	108.7 (2)	107.97
O(5)-C(27)	1.193 (4)	1.222	N(8)-S(1)-C(19)	105.80 (10)	106.84
O(6)-C(31)	1.217 (3)	1.224	C(15)-N(7)-C(18)	122.4 (3)	121.65
N(7)-C(15)	1.468 (3)	1.465	S(1)-N(8)-C(18)	130.5 (2)	130.26
N(7)-C(18)	1.318 (3)	1.353	C(26)-N(9)-C(27)	120.8 (4)	120.97
N(8)-C(18)	1.401 (3)	1.429	C(27)-N(10)-C(28)	120.2 (4)	120.30
N(9)-C(26)	1.457 (4)	1.453	C(27)-N(10)-C(31)	128.8 (4)	128.92
N(9)-C(27)	1.341 (4)	1.355	C(28)-N(10)-C(31)	111.0 (3)	110.78
N(10)-C(27)	1.408 (4)	1.414	C(11)-C(12)-C(13)	110.4 (4)	111.82
N(10)-C(28)	1.447 (4)	1.457	C(11)-C(12)-C(17)	110.4 (4)	111.62
N(10)-C(31)	1.388 (4)	1.395	C(13)-C(12)-C(17)	107.9 (3)	110.00
C(11)-C(12)	1.520 (4)	1.532	C(12)-C(13)-C(14)	113.2 (4)	112.31
C(12)-C(13)	1.502 (5)	1.538	C(13)-C(14)-C(15)	110.4 (4)	111.39
C(12)-C(17)	1.518 (4)	1.538	N(7)-C(15)-C(14)	110.1 (3)	111.82
C(13)-C(14)	1.515 (5)	1.534	N(7)-C(15)-C(16)	109.8 (3)	109.95
C(14)-C(15)	1.505 (4)	1.538	C(14)-C(15)-C(16)	110.9 (3)	110.99
C(15)-C(16)	1.502 (4)	1.534	C(15)-C(16)-C(17)	111.2 (3)	111.47
C(16)-C(17)	1.519 (4)	1.535	C(12)-C(17)-C(16)	112.1 (4)	112.58
C(19)-C(20)	1.384 (4)	1.393	O(4)-C(18)-N(7)	123.9 (4)	125.95
C(19)-C(24)	1.381 (3)	1.395	O(4)-C(18)-N(8)	117.4 (3)	118.17
C(20)-C(21)	1.368 (4)	1.392	N(7)-C(18)-N(8)	118.7 (3)	115.87
C(21)-C(22)	1.386 (4)	1.400	S(1)-C(19)-C(20)	119.6 (3)	119.74
C(22)-C(23)	1.388 (4)	1.401	S(1)-C(19)-C(24)	118.6 (3)	119.03
C(22)-C(25)	1.499 (4)	1.509	C(20)-C(19)-C(24)	121.8 (3)	121.22
C(23)-C(24)	1.384 (4)	1.390	C(19)-C(20)-C(21)	119.2 (4)	118.91
C(15)-C(16)	1.503 (4)	1.546	C(21)-C(22)-C(23)	118.7 (4)	118.54
C(18)-C(19)	1.499 (5)	1.506	C(21)-C(22)-C(25)	120.5 (4)	121.03
C(29)-C(30)	1.323 (4)	1.346	C(23)-C(22)-C(25)	120.7 (4)	120.39
C(29)-C(32)	1.494 (4)	1.493	C(22)-C(23)-C(24)	121.9 (4)	121.12
C(30)-C(31)	1.469 (4)	1.484	C(19)-C(24)-C(23)	117.4 (4)	118.99
C(30)-C(33)	1.493 (4)	1.499	C(22)-C(25)-C(26)	110.7 (3)	111.78
C(33)-C(34)	1.492 (5)	1.540	N(9)-C(26)-C(25)	111.8 (3)	113.05

Continue Table 1

Bond angles	Calculated, Å	Bond angles	Experiment [16], degree	Calculated, degree
<i>Selected dihedral angles, degree</i>		O(5)-C(27)-N(9)	125.0 (5)	125.05
C(15)-N(7)-C(18)-N(8)	173.96	O(5)-C(27)-N(10)	120.0 (5)	119.92
C(15)-N(7)-C(18)-O(4)	-4.68	N(9)-C(27)-N(10)	115.0 (4)	115.03
N(7)-C(18)-N(8)-S(1)	26.14	N(10)-C(28)-C(29)	101.5 (3)	103.24
O(4)-C(18)-H(8)-S(1)	-155.11	C(28)-C(29)-C(30)	112.0 (3)	110.34
C(18)-N(8)-S(1)-O(2)	-40.98	C(28)-C(29)-C(32)	119.3 (4)	120.46
C(18)-N(8)-S(1)-O(3)	-171.54	C(30)-C(29)-C(32)	128.6 (4)	129.20
N(7)-C(18)-N(8)-H(67)	179.28	C(29)-C(30)-C(31)	108.1 (4)	108.77
N(8)-C(18)-N(7)-H(66)	9.14	C(29)-C(30)-C(33)	131.7 (4)	130.56
C(18)-N(8)-S(1)-C(19)	74.07	C(31)-C(30)-C(33)	120.2 (4)	120.67
N(8)-S(1)-C(19)-C(20)	-91.18	O(6)-C(31)-N(10)	125.0 (4)	125.67
C(23)-C(22)-C(25)-C(26)	82.92	O(6)-C(31)-C(30)	127.6 (4)	127.46
C(22)-C(25)-C(26)-N(9)	-177.75	N(10)-C(31)-C(30)	107.4 (4)	106.87
C(25)-C(26)-N(9)-C(27)	82.75	C(30)-C(33)-C(34)	114.1 (3)	113.01
C(26)-N(9)-C(27)-O(5)	-0.06			
C(26)-N(9)-C(27)-N(10)	179.57			
N(9)-C(27)-N(10)-C(31)	0.42			
O(4)-C(18)-N(8)-H(67)	-1.97			
O(4)-C(18)-N(7)-H(66)	-169.50			
C(29)-C(30)-C(33)-C(34)	102.77			
C(21)-C(22)-C(23)-C(24)	-0.25			
C(12)-C(13)-C(14)-C(15)	55.62			
C(12)-C(17)-C(16)-C(15)	-55.01			
N(10)-C(28)-C(29)-C(30)	0.09			
O(5)-C(27)-N(9)-H(68)	178.76			

The S(1)–O(2), S(1)–O(3), N(7)–C(18), O(4)–C(18), N(8)–C(18) bond lengths were computed as 1.463, 1.456, 1.353, 1.218, and 1.429 Å in the present study and found as 1.431, 1.420, 1.318, 1.230, and 1.401 Å, respectively, in [16]. C(11)–C(12), C(29)–C(32), C(30)–C(33), and the C(33)–C(34) bond lengths between carbons were calculated as 1.532, 1.493, 1.499, and 1.540 Å in the current study, while the C(29)–C(32), C(30)–C(33), and C(33)–C(34) bond lengths were found as 1.494, 1.493, and 1.492 Å [16]. These differences in the C–C molecular bond lengths result from the exchange of electrons between two atoms.

The C(30)–C(31), C(29)–C(30), C(28)–C(29), and N(10)–C(31) bond lengths in ring 1 were calculated at the interval of 1.346–1.505 Å. The C(20)–C(21), C(21)–C(22), C(22)–C(23), C(23)–C(24), C(19)–C(24), and C(19)–C(20) bond lengths in ring 2 were calculated at the interval of 1.390–1.401 Å. The C(15)–C(16), C(16)–C(17), C(12)–C(17), C(12)–C(13), and C(13)–C(14) bond lengths in ring 3 were calculated at the interval of 1.533–1.538 Å. The C(19)–S(1), C(22)–C(25), S(1)–N(8) bond lengths were calculated as 1.795, 1.509, 1.69 Å, while they were found as 1.759, 1.499, and 1.643 Å, respectively, in [16].

As the shortest bonds in the molecule, O(4)–C(18), O(5)–C(27), and O(6)–C(31) were calculated as 1.217, 1.222, and 1.224 Å in the present study and recorded as 1.230, 1.193, and 1.217 Å [16]. As the longest bonds in the molecule, S(1)–N(8) and S(1)–C(19) were respectively calculated as 1.691 and 1.794 Å in the present study and measured as 1.643 and 1.759 Å [16].

The C34–C33–C30–C31 and C32–C29–C30–C31 dihedral angles in ring 1 of the mentioned compound were calculated as 76.53° and 179.98°. Similarly, the C26–C25–C22–C21 and C26–C25–C22–C23 dihedral angles in ring 2 were calculated as 94.64° and 82.92°. The C11–C12–C17–C16 and C11–C12–C13–C14 dihedral angles on ring 3 were calculated as 178.93° and 179.11°. Additionally, the C(19)–S(1)–O(2), C(19)–S(1)–O(3), C(19)–S(1)–N(8), S(1)–N(8)–C(18), N(8)–C(18)–N(7), N(8)–C(18)–O(4), C(18)–N(7)–C(15), N(9)–C(27)–N(10), O(2)–S(1)–O(3), and C(26)–N(9)–C(27) bond angles were calculated as 107.94°, 107.97°, 106.84°, 130.25°, 115.86°, 118.16°, 121.65°, 115.03°, 122.20°, and 120.97°, respectively. The angles C(19)–S(1)–O(2), C(19)–S(1)–O(3), C(19)–S(1)–N(8), S(1)–N(8)–C(18), N(8)–C(18)–N(7), N(8)–C(18)–O(4), and C(18)–N(7)–C(15) were given as 108.1°, 108.7°, 105.8°, 130.5°, 118.7°, 117.4°, and 122.4° in [16].

Vibrational frequency analyses. In the following discussion, the glimepiride molecule is experimentally examined and the observed and calculated vibrational frequencies, calculated FT-IR intensities, Raman scattering activities and vibrational assignments of the title molecule are given in Table 2. The computations of harmonic wavenumbers, IR intensities, and Raman activities were performed with the B3LYP/6-311++G(d,p) level. Scaling factors were used for theoretical vibrational wavenumbers. The computed vibrational wavenumbers were scaled as 0.983 for frequencies less than 1700 cm^{-1} and 0.958 for frequencies higher than 1700 cm^{-1} at the B3LYP/6-311++G(d,p) basis set [37]. The linear correlation coefficient values (R^2) between the experimental and computed vibrational frequencies were found as 0.9987 for IR wavenumbers and 0.9994 for Raman. The experimental and simulated IR and Raman spectra of the title compound are given in Fig. 2 and 3. In the present research, N–H, C–H, C–O, C–C, C–N and SO_2 vibrations were examined. As seen from Table 2, the experimental and calculated vibrational wavenumbers are in good agreement.

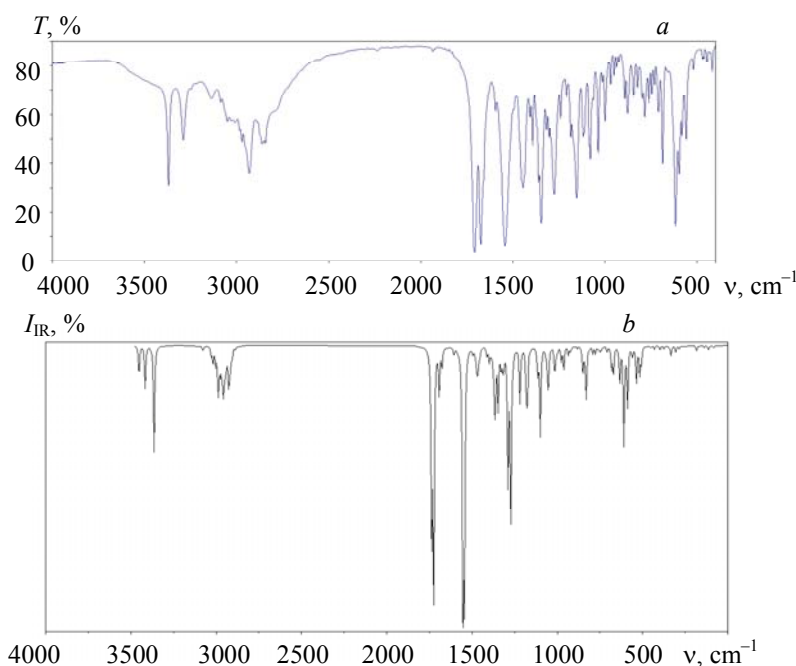


Fig. 2. The experimental (a) and simulated (b) FT-IR spectra of glimepiride.

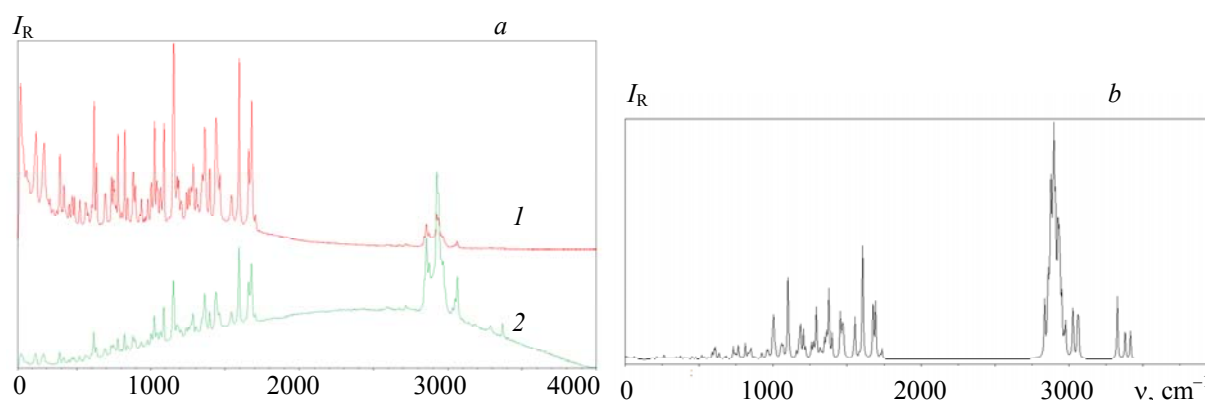


Fig. 3. The experimental (a) recorded with 785 nm line of the diode laser (1) and 514 nm line of the diode laser (2) and the simulated (b) Raman spectra of glimepiride.

N–H vibrations. The N–H stretching vibration of amines and amides appears within $3300\text{--}3500\text{ cm}^{-1}$ (weak bands) and $3200\text{--}3470\text{ cm}^{-1}$ (strong bands) regions [38]. In the present case, NH stretching modes are obtained at 3135 , 3289 , and 3369 cm^{-1} in the IR spectrum and 3188 , 3292 , and 3372 cm^{-1} in the laser-Raman spectrum. These modes are calculated at 3343.96 , 3394.95 , and 3430.09 cm^{-1} .

TABLE 2. The Experimental and Calculated Vibrational Frequencies (ν , cm^{-1}) and their Assignments of Glimepiride

Assignments	ν_{exp}		Calculated B3LYP/6-311++G(d,p)			
	IR	Raman	Unscaled freq.	Scaled freq.	IR int.	Raman act.
ν_{NH}	3369	3372	3580.47	3430.09	63.503	70.942
ν_{NH}	3289	3292	3543.79	3394.95	91.545	74.404
ν_{NH}	3135	3188	3490.56	3343.96	226.609	154.058
ν_{CH} in ring 2	3087	3072	3208.22	3073.48	0.914	91.211
ν_{CH} in ring 2	3050	3051	3200.75	3066.32	0.918	76.029
ν_{CH} in ring 2	3030	3033	3171.19	3038.00	4.085	78.400
ν_{CH} in ring 2	3008		3166.95	3033.94	7.875	62.340
$\nu_{\text{as}}\text{CH}_3+\nu_{\text{as}}\text{CH}_2$		2977	3108.98	2978.40	24.694	25.180
$\nu_{\text{as}}\text{CH}_2$	2971		3108.54	2977.98	11.664	8.534
$\nu_{\text{as}}\text{CH}_3+\nu_{\text{as}}\text{CH}_2$			3093.05	2963.15	36.199	113.579
$(\nu_{\text{as}}\text{CH}_2+\nu_{\text{as}}\text{CH}_3)$ in ring 3		2946	3076.41	2947.20	62.184	28.021
$(\nu_{\text{CH}}+\nu_{\text{as}}\text{CH}_2)$ in ring 3		2934	3064.55	2935.84	24.758	40.411
$(\nu_{\text{as}}\text{CH}_2+\nu_{\text{as}}\text{CH}_3)$ in ring 1	2931		3061.09	2932.52	0.486	15.345
$\nu_{\text{s}}\text{CH}_2$ in ring 3	2977		3002.61	2876.50	18.323	45.333
$\nu_{\text{s}}\text{CH}_2$ in ring 3		2881	2998.73	2872.78	4.161	120.069
$\nu_{\text{s}}\text{CH}_2$ in ring 3	2862	2863	2993.75	2868.01	18.781	26.464
ν_{CH} in ring 3	2843	2851	2975.33	2850.36	5.573	120.975
$\nu_{\text{O}_4}=\text{C}_{18}+\delta\text{HNC}$	1707	1707	1766.82	1692.61	421.975	16.173
$\nu_{\text{O}_5}=\text{C}_{27}+\nu_{\text{O}_6}=\text{C}_{31}+\delta\text{HNC}$	1675	1682	1754.86	1681.16	550.133	6.865
$\nu_{\text{O}_6}=\text{C}_{31}+\nu_{\text{O}_5}=\text{C}_{27}$		1661	1722.18	1649.85	99.547	85.082
$\nu_{\text{C}=\text{C}}$ in ring 1			1705.32	1633.70	40.405	95.112
$[\nu_{\text{CC}}+\delta\text{HCC}]$ in ring 2	1595	1598	1633.86	1606.09	15.621	186.631
$\delta\text{HNC}+\delta\text{HCN}+\nu_{\text{N}_7}\text{C}_{18}$	1543	1546	1571.75	1545.03	494.281	12.762
$\delta_{\text{s}}\text{CH}_2+\delta_{\text{s}}\text{CH}_3$		1467	1492.80	1467.42	5.269	0.573
$\delta_{\text{s}}\text{CH}_2+\delta_{\text{s}}\text{CH}_3$	1445	1441	1478.52	1453.38	2.033	10.266
$[\delta\text{HCC}+\nu_{\text{CC}}]$ in ring 2+tCH ₂	1407		1437.30	1412.87	18.849	0.196
$\delta_{\text{s}}\text{CH}_3$ (sym. bending)		1399	1423.44	1399.24	30.174	33.404
$\delta_{\text{s}}\text{CH}_3$ (sym. bending)+wCH ₂	1393		1413.99	1389.95	8.205	0.117
$\delta\text{HNC}+\text{wCH}_2$		1364	1390.53	1366.89	115.150	3.551
wCH ₂ in ring 1+[$\nu_{\text{CC}}+\nu_{\text{NC}}$] in ring 1	1360		1385.35	1361.80	76.150	26.805
$[\nu_{\text{CC}}+\nu_{\text{NC}}]$ in ring 1+ $\nu_{\text{C}_{30}\text{C}_{33}}$ + + $\delta_{\text{s}}\text{CH}_3$ (sym. bending)+ wCH ₂ in ring 1	1346	1340	1370.26	1346.97	127.161	24.216
tCH ₂ + $[\delta\text{HCC}+\nu_{\text{CC}}]$ in ring 2		1332	1354.63	1331.60	9.752	6.929
$[\text{wCH}_2+\text{tCH}_2+\delta\text{HCC}]$ in ring 3	1317		1339.23	1316.46	0.085	2.027
$[\delta\text{HCC}+\nu_{\text{CC}}]$ in ring 2	1303	1307	1329.99	1307.38	0.188	0.760
$\nu_{\text{N}_{7,8}}\text{C}_{18}+\delta\text{HNC}+\nu_{\text{as}}\text{SO}_2+\delta\text{HCC}$ in ring 3+ +wCH ₂		1287	1311.93	1289.63	260.607	8.041
ν_{NC} in ring 1+ $\nu_{\text{N}_{9,10}}\text{C}_{27}+\delta\text{HNC}$	1275		1294.68	1272.67	366.211	20.130
$[\text{tCH}_2+\delta\text{HCC}]$ in ring 3		1261	1281.78	1259.99	6.531	1.645
$[\text{tCH}_2+\delta\text{HCC}]$ in ring 3		1252	1281.15	1259.37	9.934	19.481
$[\text{tCH}_2+\delta\text{HCC}]$ in ring 3	1242	1241	1249.19	1227.95	0.399	0.271
$\delta\text{HNC}+\nu_{\text{N}_{7,8}}\text{C}_{18}+\text{tCH}_2$ in ring 3			1240.83	1219.74	114.254	13.948
tCH ₂	1209		1235.04	1214.05	10.310	1.937
$\nu_{\text{C}_{22}-\text{CH}_2}+\text{wCH}_2+[\delta\text{HCC}+\nu_{\text{CC}}]$ in ring 2+ + δHNC		1205	1225.45	1204.62	1.966	38.083
δHCC in ring 2	1185	1186	1206.47	1185.96	15.896	23.258
tCH ₂ in ring 1		1178	1200.45	1180.04	6.346	7.361
$[\delta\text{CCC}+\rho\text{CH}_2+\text{tCH}_2]$ in ring 3	1154	1155	1177.33	1157.31	3.225	10.112
δHCC in ring 2	1117		1138.97	1119.61	10.966	0.180
$\nu_{\text{s}}\text{SO}_2+\nu_{\text{SC}}+[\nu_{\text{CC}}+\delta\text{HCC}]$ in ring 2		1089	1119.05	1100.02	186.163	128.556
$[\text{tCH}_2+\nu_{\text{CC}}+\delta\text{HCC}]$ in ring 3	1079		1108.43	1089.59	3.180	0.789
$\nu_{\text{C}_{12}-\text{CH}_3}+[\nu_{\text{CC}}+\delta\text{HCC}+\text{wCH}_2]$ in ring 3	1075		1087.12	1068.64	6.771	10.888
$\rho\text{CH}_3+\nu_{\text{CH}_2-\text{CH}_3}$	1064	1064	1084.77	1066.33	7.825	4.650

Continue Table 2

Assignments	ν_{exp}		Calculated B3LYP/6-311++G(d,p)			
	IR	Raman	Unscaled freq.	Scaled freq.	IR int.	Raman act.
$\nu_s\text{SO}_2+\nu\text{SC}+[\nu\text{CC}+\delta\text{HCC}]$ in ring 2			1071.35	1053.13	78.283	8.323
$t\text{CH}_3+\rho\text{CH}_3+\delta\text{HCC}$ in ring 2	1036	1040	1065.58	1047.46	5.247	6.299
$[\nu\text{CC}+w\text{CH}_2+\rho\text{CH}_3]$ in ring 3+ $\nu\text{N}_{7,8}\text{C}_{18}$		1025	1033.32	1015.75	53.553	10.565
$[\delta\text{CCC}+\nu\text{CC}]$ in ring 2	1015		1028.89	1011.40	10.451	2.385
$\nu\text{CH}_2-\text{CH}_2$	1000	1004	1021.52	1004.16	8.342	54.531
τHCCC in ring 2	986	980	994.47	977.56	7.961	1.253
τHCCC in ring 2+ $[\delta\text{HCC}+t\text{CH}_2+\rho\text{CH}_2]$ in ring 3	970		994.07	977.17	24.081	0.497
$\nu\text{CH}_2-\text{CH}_3+\rho\text{CH}_3$		966	983.57	966.85	1.688	9.034
τHCCC in ring 2	951	951	973.32	956.77	0.983	11.017
$[\rho\text{CH}_2+\nu\text{CC}+\delta\text{HCC}+\rho\text{CH}_3]$ in ring 3	936	937	951.64	935.46	18.688	1.162
$[\rho\text{CH}_2+\rho\text{CH}_3]$ in ring 1	924	926	941.92	925.91	3.215	2.599
$[\rho\text{CH}_2+\nu\text{CC}+\delta\text{HCC}+\rho\text{CH}_3]$ in ring 3	892	885	897.73	882.47	5.111	2.536
$\rho\text{CH}_2+\rho\text{CH}_3+\nu\text{N}_{10}\text{C}_{27}+[\nu\text{CC}+\nu\text{NC}]$ in ring 1	878	882	886.73	871.66	0.530	3.317
τHCCC in ring 2	845	843	858.14	843.55	7.370	5.511
τHCCC in ring 2+ νSN	823	824	845.00	830.64	105.440	7.294
$[\tau\text{CCCC}+\tau\text{HCCC}]$ in ring 2+ $\nu\text{C}_{22}\text{C}_{25}$		803	825.99	811.95	4.251	20.516
$\rho\text{CH}_2+\rho\text{CH}_3$	798		805.92	792.22	17.505	0.507
ρCH_2 in ring 3	784	780	793.80	780.31	0.057	1.483
$[\delta\text{CCC}+\nu\text{CC}+\rho\text{CH}_2+\rho\text{CH}_3]$ in ring 3	763	765	778.26	765.03	1.814	18.708
$\gamma\text{N}_5\text{N}_{10}\text{O}_5\text{C}_{27}+\rho\text{CH}_2$		757	771.40	758.28	6.194	1.638
$\rho\text{CH}_2+\rho\text{CH}_3$		750	763.04	750.07	2.664	0.693
$\gamma\text{N}_7\text{N}_8\text{O}_4\text{C}_{18}+\rho\text{CH}_2$	747	747	762.04	749.08	7.904	4.011
$\gamma\text{C}_{21}\text{C}_{22}\text{C}_{25}\text{C}_{22}+\gamma\text{S}_1\text{C}_{20}\text{C}_{24}\text{C}_{19}$			754.02	741.20	6.899	5.323
$[\tau\text{CCCC}+\tau\text{HCCC}]$ in ring 2+ ρCH_2	732	731	743.11	730.48	1.590	15.710
$\rho\text{CH}_2+\delta\text{C}_{26}\text{N}_6\text{C}_{27}+\delta\text{ring1}$	710		721.33	709.07	13.549	0.222
$\delta\text{N}_7\text{C}_{18}\text{N}_8+[\delta\text{CCC}+\rho\text{CH}_2]$ in ring 3	688	692	694.04	682.24	47.856	3.805
$\nu\text{SC}+\delta\text{CCC}$ in ring 2+ $\delta\text{C}_{25}\text{C}_{26}\text{N}_9$	660		682.69	671.09	60.382	2.569
$\tau\text{HNCN}+\delta\text{CCC}$ in ring 2			646.10	635.11	9.284	5.221
τHNCN		633	644.62	633.66	71.269	3.285
τHNCN	617	617	620.60	610.05	202.574	12.992
$\tau\text{HNCN}+\delta\text{C}_{28}\text{C}_{29}\text{C}_{32}$	598	599	612.41	602.00	1.929	9.954
$\tau\text{HNCN}+[\tau\text{HCCC}+\tau\text{CCCC}]$ in ring 2+ νSN	582	578	598.68	588.50	130.282	9.368
$\delta\text{ring3}+\tau\text{HNCN}$	559	559	569.12	559.45	11.391	1.191
$\delta\text{OSO}+[\tau\text{CCCC}+\tau\text{HCCC}]$ in ring 2+ + $\delta\text{NSC}+\tau\text{HNCN}$			545.67	536.39	81.030	2.618
$\tau\text{ring1}+\tau\text{HNCN}$	520	520	529.66	520.65	1.447	1.104
$\tau\text{HNCN}+[\tau\text{CCCC}+\tau\text{HCCC}]$ in ring 2		485	516.31	507.53	35.929	0.845
$[\delta\text{CCC}+\rho\text{CH}_2]$ in ring 3	470	471	484.58	476.34	1.024	3.008
$[\delta\text{CCC}+\rho\text{CH}_2]$ in ring 3+ $\delta\text{C}_{25}\text{C}_{26}\text{N}_9$	452		462.85	454.98	2.979	1.604
$[\delta\text{CCC}+\rho\text{CH}_2]$ in ring 3	446	448	458.13	450.34	2.574	2.788
$[\delta\text{CCC}+\rho\text{CH}_2]$ in ring 3	418	413	422.73	415.54	0.050	0.391
$\rho\text{CH}_2+\delta\text{SCC}+\delta\text{C}_{25}\text{C}_{22}\text{C}_{23}$		387	404.58	397.70	8.347	2.465
$\delta\text{ring3}+\tau\text{C}_{15}\text{N}_7\text{C}_{18}\text{N}_8$		364	367.94	361.69	0.174	1.499
$\delta\text{C}_{25}\text{C}_{22}\text{C}_{21}+\rho\text{CH}_2+\delta\text{ring3}$		341	351.08	345.12	4.020	2.803
$\tau\text{O}_5\text{C}_{27}\text{N}_{10}\text{C}_{28}+\tau\text{ring1}$		318	332.85	327.19	1.642	0.871
$\tau\text{CH}_3+\rho\text{CH}_2+\rho\text{CH}_3$		280	290.65	285.71	4.402	0.348
τCH_3		225	236.53	232.50	0.120	0.425
$\tau\text{ring1}+\delta\text{C}_{30}\text{C}_{33}\text{C}_{34}$		177	185.05	181.91	1.097	0.726
$\rho\text{SO}_2+\delta\text{SCC}+\rho\text{CH}_2$		160	163.89	161.11	0.517	0.462
$\tau\text{O}_5\text{C}_{27}\text{N}_{10}\text{C}_{28}+\tau\text{ring1}$		135	142.25	139.83	4.675	0.171
—		117	120.59	118.54	3.804	0.302

Note. ν , stretching; δ , in-plane bending; δ_s , scissoring and symmetric bending; w , wagging; t , twisting; ρ , rocking; τ , torsion; γ , out-of-plane bending; I_{IR} , IR intensity (km/mol); S_{Raman} , Raman scattering activity.

C-H vibrations. In aromatic compounds, the CH stretching vibrations give rise to absorption bands in the region of 3000–3100 cm^{-1} [38–42]. The bands observed at 3008, 3030, 3050 and 3087 cm^{-1} in the IR spectrum and at 3033, 3051, and 3072 cm^{-1} in the laser-Raman spectrum can be assigned to the CH stretching vibration modes in ring 2. These bands were computed between 3033.94 and 3073.48 cm^{-1} in our calculations. The CH in-plane and out-of-plane bending vibrations in aromatic rings occur in the regions of 1000–1600 and 650–1000 cm^{-1} [38–42]. The bands combined with other vibrational modes at 1407 (IR), 1332 (R), 1303 (IR)–1307 (R), 1205 (R), 1185 (IR)–1186 (R), 1117 (R), and 1089 (R) cm^{-1} are assigned to the CH in-plane bending modes in ring 2, while the individual bands at 986 (IR)–980 (R) and 845 (IR)–843 (R) cm^{-1} correspond to the CH out-of-plane bending bands in ring 2.

C=O vibrations. The C=O stretching band in the carboxyl group gives the strong absorption band in the region of 1870–1540 cm^{-1} [41, 42]. A free carbonyl (C=O) stretching vibration is generally observed in the region of 1715–1670 cm^{-1} [43]. The C=O stretching vibrations of glimepiride were observed at 1707 and 1675 cm^{-1} in the FT-IR and at 1707, 1682, and 1661 cm^{-1} in the laser-Raman spectra. The computed values for these bands were obtained at 1693, 1681, and 1650 cm^{-1} .

C=C and C-C vibrations. Characteristic aromatic C=C stretching vibrations normally appear in the region of 1650–1430 cm^{-1} [44]. Likewise, the aromatic CC stretching vibration occurs in the region of 1589–1301 cm^{-1} [45]. In the present study, the vibrational band computed at 1634 cm^{-1} was assigned to the C=C stretching vibration in ring 1. In ring 2, the wavenumbers were observed at 1595–1015 cm^{-1} in the FT-IR spectrum, and at 1598–1089 cm^{-1} in the Laser-Raman spectrum. The C–C stretching vibrations were theoretically calculated at 1606–1011 cm^{-1} . On the other hand, the CCC in-plane bending vibrational bands in rings 2 and 3 can be assigned to the peaks at 1154 (IR)–1155 (R), 1015 (IR), 763 (IR)–765 (R), 660 (IR), 470 (IR)–471 (R), 452 (IR), 446 (IR)–448 (R), and 418 (IR)–413 (R) cm^{-1} .

CH₃ and CH₂ vibrations. Asymmetric stretching vibrations of CH₃ were expected to be in the range of 3000–2905 cm^{-1} , and symmetric stretching vibrations were observed in the range of 2870–2860 cm^{-1} [46, 47]. The asymmetric and symmetric stretching vibrations of CH₂ normally appear in the 3010–2900 and 2950–2850 cm^{-1} region, respectively [46].

The experimental and calculated wavenumbers for scissoring, twisting, and rocking modes for methyl and methylene groups are summarized in Table 2. In the present study, the CH₃ asymmetric stretching in ring 3 appeared at 2936 cm^{-1} in the laser-Raman spectra, and it was calculated at 2934 cm^{-1} . The CH₃ asymmetric stretching in ring 1 appeared at 2931 cm^{-1} in the FT-IR spectra, and it was computed at 2933 cm^{-1} .

The scissoring and symmetric bending vibrational modes of the CH₃ groups usually appear in the 1465–1370 cm^{-1} region as a medium to strong band in FT-IR and Raman spectra [48, 49]. The scissoring modes for the CH₃ and CH₂ groups were observed at 1467 (R) and 1445 (IR)–1441 (R) cm^{-1} , while they were calculated at 1467.42 and 1453.38 cm^{-1} . Likewise, the symmetric bending vibrations for methyl were recorded at 1393 cm^{-1} in the FT-IR spectra and 1399 cm^{-1} in the laser-Raman spectra. The calculated values for these bands were obtained at 1389.95 and 1399.24 cm^{-1} , respectively. The rocking vibrational frequencies are normally observed below ~1150 cm^{-1} in FT-IR and laser-Raman spectra [46, 49, 50]. In the B3LYP/6-311++G(d,p) calculation, the CH₃ rocking vibrational modes were found at 1066, 1047, 1016, 967, 935, 926, 898, 887, 806, 778, 763, and 273 cm^{-1} . These values are consistent with the experimental FT-IR values at 1064, 1036, 936, 924, 892, 878, 798, and 763 cm^{-1} and with the laser-Raman value at 1064, 1040, 1025, 966, 937, 926, 885, 882, 765, and 750 cm^{-1} . Torsional vibration modes were observed at scaled 269 and 233 cm^{-1} by the B3LYP/6-311++G(d,p) calculation, and the observed frequency value (233 cm^{-1}) is consistent with the experimental laser-Raman value (225 cm^{-1}).

The stretching vibrations and deformation modes (scissoring, wagging, twisting, and rocking) associated with the CH₂ group appear in the regions of 3020–2855 and 1450–850 cm^{-1} [38, 40, 46, 51]. In the present study, the CH₂ asymmetric stretching in ring 3 appeared at 2977, 2934, and 2881 cm^{-1} in the laser-Raman spectra and the calculated frequencies were obtained at 2978, 2936, and 2873 cm^{-1} . The CH₂ asymmetric stretching in ring 1 appeared at 2931 cm^{-1} in the FT-IR spectra and the calculated frequency was obtained at 2933 cm^{-1} . The CH₂ asymmetric stretching in ring 3 appeared at 2863 cm^{-1} in the laser-Raman spectra and at 2862 cm^{-1} in the FT-IR spectra, whereas the calculated frequency was obtained at 2868 cm^{-1} . The deformation modes of the CH₂ groups were observed at 1445, 1346, 1317, 1154, 1075, 1064, 1000, 970, 936, 924, 892, 878, 798, 784, 763, 747, 732, 710, 470, 452, 446, and 418 cm^{-1} in the FT-IR spectrum and at 1441, 1340, 1287, 1261, 1252, 1241, 1205, 1178, 1155, 1064, 1004, 966, 937, 926, 885, 882, 780, 765, 757, 750, 747, 731, 471, 448, 413, and 341 cm^{-1} in the laser-Raman spectrum. These modes were given by the DFT calculations in the range of 1453–269 cm^{-1} as expected.

C–N, S–N, S–C, and SO₂ vibrations. The determination of position of CN stretching bands is very difficult due to the presence of other vibrational bands in the fingerprint region. The vibrational assignments of CN bands are performed using the GaussView5 molecular visualization program. The C–N stretching vibration was reported in the region of 1382–1213 cm⁻¹ for several compound types [52]. The bands observed at 1360 (IR), 1346 (IR)–1340 (R), and 1275 (IR) cm⁻¹ can be assigned to the CN stretching modes. The other CN vibrations in the title molecule are listed in Table 2. S–N and S–C stretching bands were recorded at 823 (IR)–824 (R) cm⁻¹ and 660 (IR) cm⁻¹. They are computed at 830.64 and 671.09 cm⁻¹, respectively. The band observed at 1287 cm⁻¹ in the Laser-Raman spectrum is assigned to an asymmetric stretching mode of the SO₂ group. The computed value of this band is obtained at 1289.63 cm⁻¹. Likewise, the symmetric SO₂ stretching mode is recorded at 1089 cm⁻¹ in the laser-Raman spectra, while it is calculated at 1100.02 and 1053.13 cm⁻¹. The in-plane bending vibration (δ OSO) of the SO₂ group is computed at 536.39 cm⁻¹.

¹H and ¹³C NMR chemical shift analyses. NMR analysis, used in organic structure determination, is associated with the spin orientation direction. The ¹H and ¹³C NMR chemical shifts calculated with the gauge-including atomic orbital (GIAO) approach using the Gaussian09 software [31] show good agreement with the experimental chemical shifts.

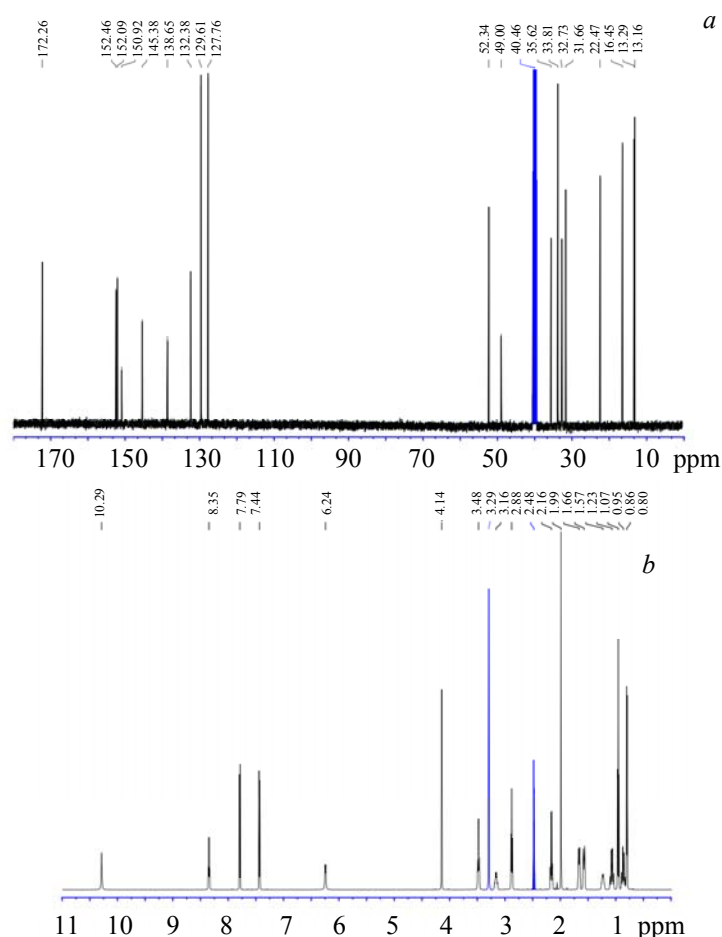


Fig. 4. The experimental ¹³C (a) and ¹H (b) NMR chemical shift spectra of glimepiride.

Figure 4 shows the experimental ¹H and ¹³C NMR chemical shift spectra of glimepiride. The experimental ¹H and ¹³C chemical shift values measured in a DMSO solvent and the calculated chemical shift values at the B3LYP/6-311++G(d,p) level in vacuum and the DMSO solvent are shown in Table 3. The ¹H chemical shift values were computed at the intervals of 0.60–8.44 ppm in vacuum and 0.55–8.32 ppm in DMSO. The experimental chemical shifts of ¹H are measured in the range of 0.80–10.29 ppm. The largest deviation between the calculated and experimental ¹H NMR chemical shifts ($\delta_{\text{exp}} - \delta_{\text{cal}}$) is seen for H66 with 2.00 ppm, whereas the smallest deviations are seen for H60 with –0.04 ppm and H65 with –0.04 ppm. The

chemical shifts for H39, H40, H41, H50, H51, H52, H56, H58, H59, and H60 are experimentally located at 0.86, 0.86, 1.23, 1.07, 7.79, 7.44, 2.88, 3.48, 4.14, and 4.14 ppm, respectively. The chemical shift values computed for these atoms are calculated at 1.01 ppm (error approx. -0.15 ppm), 1.01 (-0.15), 1.33 (-0.1), 1.00 (0.07), 7.96 (-0.17), 7.59 (-0.15), 3.01 (-0.13), 3.6 (-0.12), 4.23 (-0.09), and 4.18 ppm (-0.04 ppm), respectively. H66 (8.35 ppm), H67 (6.24 ppm), and H68 (10.29 ppm) hydrogen atoms have high signal values and they were calculated as 6.35, 5.68 and 8.44 ppm, respectively. H51, H52, H53, and H54 atoms in a phenyl ring generate resonance signal within 7.96–8.06 ppm range.

TABLE 3. The Experimental and Computed ^1H and ^{13}C NMR Isotropic Chemical Shifts (δ , ppm) for Glimepiride (with respect to TMS)

Atom	δ_{exp} (in DMSO- d_6)	δ_{cal} (in vacuum)	δ_{cal} (in DMSO)	Atom	δ_{exp} (in DMSO- d_6)	δ_{cal} (in vacuum)	δ_{cal} (in DMSO)
C11	22.47	23.60	23.09	H40	0.86	0.98	1.01
C12	31.66	36.08	35.69	H41	1.23	1.26	1.33
C13	32.73	37.65	37.36	H42	0.86	0.98	0.99
C14	31.66	36.12	35.76	H43	0.86	1.61	1.64
C15	49.00	52.24	52.82	H44	1.66	1.97	1.80
C16	31.66	35.30	34.61	H45	1.66	0.97	1.12
C17	32.73	37.29	36.88	H46	3.16	3.55	3.48
C18	150.92	153.48	154.80	H47	1.57	1.79	1.89
C19	138.65	150.09	148.87	H48	1.57	1.25	1.38
C20	127.76	131.56	131.39	H49	1.07	1.66	1.71
C21	129.61	133.36	134.89	H50	1.07	0.98	1.00
C22	145.38	152.28	154.13	H51	7.79	7.87	7.96
C23	129.61	135.46	136.02	H52	7.44	7.28	7.59
C24	127.76	131.55	131.19	H53	7.44	7.87	7.97
C25	33.81	41.12	40.60	H54	7.79	8.03	8.06
C26	35.62	46.30	45.98	H55	2.88	2.41	2.66
C27	152.09	155.65	156.88	H56	2.88	3.11	3.01
C28	52.34	55.18	55.28	H57	3.48	2.76	2.99
C29	152.46	157.74	162.62	H58	3.48	3.72	3.60
C30	132.38	142.28	140.60	H59	4.14	4.14	4.23
C31	172.26	176.79	178.48	H60	4.14	4.10	4.18
C32	13.16	12.67	12.80	H61	2.16	2.11	1.99
C33	16.45	20.39	19.98	H62	2.16	2.31	2.54
C34	13.29	13.61	13.35	H63	1.99	1.81	1.95
H35	0.80	1.01	1.02	H64	1.99	2.26	2.34
H36	0.80	1.09	1.07	H65	1.99	1.81	1.95
H37	0.80	0.61	0.60	H66	8.35	6.14	6.35
H38	0.97	0.55	0.66	H67	6.24	5.36	5.68
H39	0.86	1.23	1.01	H68	10.29	8.32	8.44

The ^{13}C chemical shifts are calculated in the range of 12.80–178.48 in DMSO ppm and 12.67–176.79 ppm in vacuum, while they are experimentally recorded in the range of 13.16–172.26 ppm. The largest deviation between the calculated and experimental ^{13}C NMR chemical shifts ($\delta_{\text{exp}} - \delta_{\text{cal}}$) is obtained for C26 with -10.36 ppm, whereas the smallest deviation is found for C34 with -0.06 ppm. The carbon atoms of methyl and methylene groups that do not have a bond with any electronegative atom give NMR signals in the region of 15–55 ppm, due to the shielding by their hydrogen atoms [40]. In this connection, the NMR signals for C11–C17, C25, C26, C28, and C32–C34 carbons were recorded at the interval of 13.16–52.34 ppm and calculated at the intervals of 12.67–55.18 ppm in vacuum and 12.80–55.28 ppm in DMSO. The carbon atoms (C19–C24) of the aromatic ring (ring 2) gave a signal within the range of 127.76–145.38 ppm and they were calculated at the interval of 131.19–154.13 ppm. The chemical shifts for C31, C27, and C18 atoms, bound to electronegative atoms, were respectively measured as 178.48, 156.88, and 154.80 ppm. The ^{13}C chemical shift values for C29 and C30 atoms with sp^2 hybrid in ring 1 are recorded at 152.46 and 132.38 ppm and computed at 162.62 and 140.60 ppm in DMSO, respectively. The correlation coefficient (R^2) values

between the experimental and calculated ^1H and ^{13}C NMR isotropic chemical shifts are 0.99818 and 0.95975 (in vacuum) and 0.99778 and 0.95253 (in DMSO), respectively.

Conclusion. In the present study, the molecular structure, vibrational frequencies and NMR analysis results of glimepiride molecule were examined using both experimental (FT-IR, Laser-Raman and ^1H and ^{13}C NMR chemical shifts) and theoretical (DFT/B3LYP/6-311++G(d,p) level) methods. The experimental spectral results are in very good agreement with the computed data. The calculated results of the bond lengths and angles are consistent with X-ray data in the literature. Furthermore, we can state that the present work can be useful in studies on other anti-diabetic drugs in the sulfonyl urea group as well.

Acknowledgment. The authors are thankful to Pharmacist Mr. Ali Ünsal Keskiner for helpful discussions, and Health Services Vocational School of Bartın University for the simulation calculations.

REFERENCES

1. Türkiye Endokrinoloji ve Metabolizma Derneği. Diabetes Mellitus ve Komplikasyonlarının Tanı, Tedavive İzlem Kılavuzu, BAYT Bilimsel Araştırmalar Basın Yayınve Tanıtım Ltd. Şti, Miki Matbaacılık San. ve Tic. Ltd. Şti (2014).
2. American Diabetes Association. *Diabetes Care*, **33**, 62 (2010).
3. *Expert Committee on the Diagnosis and Classification of Diabetes Mellitus Diabetes Care*, **20**, 1183 (1997).
4. P. R. Njolstad, J. V. Sagen, L. Bjorkhaug, S. Odili, N. Shehadeh, D. Bakry, U. Sarici, F. Alpay, J. Molnes, A. Molven, O. Sovik, F. M. Matschinsky, *Diabetes*, **52**, 11, 2854 (2003).
5. P. Odetti, S. Garibaldi, G. Noberasco, I. Aragno, S. Valentini, N. Traverso, U. M. Marinari, *Acta Diabetol.*, **36**, 4, 179 (1999).
6. U. Çakatay, *Diabetes and Metabolism*, **31**, 6, 551 (2005).
7. T. Hamaguchi, T. Hirose, H. Asakawa, Y. Itoh, K. Kamado, K. Tokunaga, K. Tomita, H. Masuda, N. Watanabe, M. Namba, *Diabetes Res. Clin. Pract.*, **66**, 129 (2004).
8. A. Brayfield, *Martindale: The Complete Drug Reference*, 35 ed., CD ROM, The Pharmaceutical Press, London (2007).
9. <http://www.sanofi-aventis.com/products/en/amaryl.pdf> (accessed 10.09.09).
10. S. N. Davis, *J. Diabetes Complicat.*, **18**, No. 6, 367 (2004).
11. T. G. Skillman, J. M. Feldman, *Am. J. Med.*, **70**, 361 (1981).
12. H. E. Lebovitz, M. N. Feinglos, *Diabetes Care*, **1**, 189 (1978).
13. G. Arumugam, P. Manjula, N. Paari, *J. Acute Disease*, **3**, No. 2, 196 (2013).
14. M. Remko, *J. Mol. Struct. Theochem.*, **897**, 73 (2009).
15. M. Karakaya, M. Kurekci, B. Eskiuyurt, Y. Sert, C. Çırak, *Spectrochim. Acta, A*, **135**, 137 (2015).
16. M. Iwata, H. Nagase, T. Endo, H. Ueda, *Acta Crystallogr.*, **C53**, 329 (1997).
17. L. A. D. Maria Lestari, G. Indrayanto, *Profiles of Drug Substances, Excipients, and Related Methodology*, **36**, 1871 (2011).
18. M. J. O'Neil, *The Merck Index*, Merck & Co., Inc., New Jersey (2001).
19. M. Karakaya, Y. Sert, M. Kürekçi, B. Eskiuyurt, Ç. Çırak, *J. Mol. Struct.*, **87**, 1095 (2015).
20. R. Anitha, M. Gunasekaran, S. Suresh Kumar, S. Athimoolam, B. Sridhar, *Spectrochim. Acta, A*, **150**, 488 (2015).
21. Y. Sert, B. Mirosław, Ç. Çırak, H. Doğan, D. Szulczyk, M. Struga, *Spectrochim. Acta A*, **128**, 91 (2014).
22. F. A. M. Al-Omary, M. Karakaya, Y. Sert, N. G. Haress, A. A. El-Emam, Ç. Çırak, *J. Mol. Struct.*, **1076**, 664 (2014).
23. E. Taşal, M. Kumalar, *Spectrochim. Acta A*, **95**, 282 (2012).
24. R. Brause, H. Fricke, M. Gerhards, R. Weinkauff, K. Kleinerhanns, *Chem. Phys.*, **43**, 327 (2006).
25. S. Murugavel, C. S. Jacob, P. Stephen, R. Subashini, H. R. Reddy, D. Krishnan, *J. Mol. Struct.*, **134**, 1122 (2016).
26. A. Barakat, S. M. Soliman, A. M. Al-Majid, G. Lotfy, H. A. Ghabbour, H. K. Fun, S. Yousuf, M. I. Choudhary, A. Wadood, *J. Mol. Struct.*, **365**, 1098 (2015).
27. H. Gökçe, N. Öztürk, Ü. Ceylan, Y. Alpaslan, B. Alpaslan, *Spectrochim. Acta, A*, **163**, 170 (2016).
28. A. D. Becke, *J. Chem. Phys.*, **98**, 5648 (1993).
29. C. Lee, W. Yang, R. G. Parr, *Phys. Rev. B*, **37**, 785 (1988).
30. A. Frish, A. B. Nielsen, A. J. Holder, *Gauss View User Manual*, Gaussian Inc., Pittsburg, PA (2001).

31. *Gaussian 09, Revision, A.1*, Gaussian Inc., Wallingford CT (2009).
32. http://www.gaussian.com/g_prod/gv5.htm (accessed 10.08.2016).
33. Y. B. S. Rao, M. V. S. Prasad, N. U. Sri, V. Veeraiah, *J. Mol. Struct.*, **567**, 1108 (2016).
34. G. Keresztury, S. Holly, J. Varga, G. Besenyei, A. Y. Wang, J. R. Durig, *Spectrochim. Acta, A*, **49**, 2007(1993).
35. G. Keresztury, In: *Raman Spectroscopy: Theory in Handbook of Vibrational Spectroscopy*, Eds. J. M. Chalmers, P. R. Griffith, John Wiley&Sons Ltd., New York (2002).
36. J. Chocholousova, V. V. Spirko, P. Hobza, *Chem. Phys.*, **6**, 37 (2004).
37. N. Sundaaraganesan, S. Ilakiamani, H. Saleem, P. M. Wojciechowski, D. Michalska, *Spectrochim. Acta, A*, **61**, 2995 (2005).
38. N. B. Colthup, L. H. Daly, E. Wiberley, *Introduction to Infrared and Raman Spectroscopy*, Academic Press, New York (1964).
39. L. J. Bellamy, *The Infrared Spectra of Complex Molecules*, 3rd ed., Willey, New York (1975).
40. R. M. Silverstein, F. X. Webster, *Spectroscopic Identification of Organic Compound*, Willey, New York (1998).
41. J. B. Lambert, H. F. Shurvell, R. G. Cooks, *Introduction to Organic Spectroscopy*, Macmillan, New York (1987).
42. B. H. Stuart, *Infrared Spectroscopy: Fundamentals and Applications*, Willey, New York (2004).
43. M. Barthes, G. De Nunzio, G. Riber, *Synth. Methods*, **76**, 337 (1996).
44. S. Gunasekaran, P. Arunbalaji, S. Seshadri, S. Muthu, *Indian J. Pure Appl. Phys.*, **46**, 162 (2008).
45. G. Varsanyi, S. Szoke, *Vibrational Spectra of Benzene Derivatives*, Academic Press, New York (1969).
46. N. P. G. Roeges, *A Guide to the Complete Interpretation of Infrared Spectra of Organic Structures*, Willey, New York (1994).
47. K. R. Ambujakshan, V. S. Madhavan, H. T. Varghese, C. Y. Panicker, O. Temizarpaci, B. Tekiner-Gulbas, I. Yildiz, *Spectrochim. Acta, A*, **69**, 782 (2008).
48. G. Varsanyi, *Assignments for Vibrational Spectra of Seven Hundred Benzene Derivatives*, Vol. **I, II**, Academic Kiado, Budapest (1973).
49. B. Smith, *Infrared Spectral Interpretation - A Systematic Way*, CRC Press, New York (1999).
50. J. Swaminathan, M. Ramalingam, V. Sethuraman, N. Sundaraganesan, S. Sebastain, *Spectrochim. Acta A*, **73**, 593 (2009).
51. G. Socrates, *Infrared Characteristic Group Frequencies*, Willey, New York (1981).
52. M. S. Alam, D.-U. Lee, *J. Mol. Struct.*, **174**, 1128 (2017).